# Tensile creep and recovery in ultra-high modulus linear polyethylenes

**M. A. Wilding and I. M. Ward**
*Department of Physics, University of Leeds, Leeds LS2 9JT, UK*
*(Received 1 November 1977; revised 31 January 1978)*

The tensile creep and recovery of oriented linear polyethylene (LPE) monofilaments have been studied for a range of samples of different structure. Starting with a comparison of samples of different draw ratio prepared from one grade of polymer, the measurements were extended to examine the effects of molecular weight. Although the viscoelastic behaviour is markedly non-linear it was found valuable to model the creep and recovery at each level of stress by a simple linear solid representation. This representation enabled a clear distinction to be made between recoverable and irrecoverable creep, both of which are affected by draw ratio and molecular weight. When the irrecoverable creep was examined further in terms of an activated Eyring process, a clear distinction between the two molecular weight grades could be made. In particular, the high molecular weight grade displayed a critical stress below which irrecoverable creep fell to a negligible level. This finding could be of considerable importance with regard to the application of ultra-high modulus LPE fibres in reinforcement.

## INTRODUCTION

In a number of previous publications from this laboratory the preparation and properties of ultra-high modulus polyethylenes have been described[1–4]. The discussion of the mechanical properties has so far been almost entirely confined either to the determination of the 10 sec isochronal creep modulus[1,2] or the dynamic mechanical behaviour in extension[5], both measured at very low strains, usually 0.1% or lower. Under such test conditions, the Young's modulus was shown to be uniquely related to the draw ratio, a result which confirmed previous findings on lower draw ratio polyethylenes[6]. There was, however, evidence from the initial work that these materials show non-linear viscoelastic behaviour[1], and preliminary studies have indicated that the creep behaviour at high strains depends on the polymer molecular weight as well as the draw ratio[7]. Particularly in view of the possible commercial applications of these materials for fibre reinforcement, it was therefore of interest to examine their creep and recovery behaviour in some detail. In this paper we describe a successful attempt to model the non-linear viscoelastic behaviour in a very simple fashion, which also reveals the effects of draw ratio and molecular weight in a manner which allows us to gain some physical understanding of the factors involved.

## EXPERIMENTAL

### *Preparation of samples*

Samples were prepared from two commercial grades of linear polyethylene, both manufactured by BP Chemicals International Ltd, and the number- and weight-average molecular weights are given in *Table 1*. In all cases continuous monofilaments ~0.7–1.0 mm in diameter were produced by melt spinning at 210°C. The monofilament was crystallized by passing it into a glycerol bath at 120°C as it emerged from the die of the melt extruder. The spun monofilament was subsequently drawn by stretching between moving rollers which passed the monofilament through a glycerol bath at 120°C. This draw temperature is higher than that used in previously reported non-continuous drawing procedures for LPE in this laboratory[1,2], and has the effect of lowering somewhat the creep modulus for a given draw ratio.

### *Creep measurements*

Tensile creep and recovery measurements were performed using the conventional dead-loading apparatus similar to that described in previous publications[8], in which the strain was calculated from grip displacement. It will be shown that this is an adequate procedure provided that sufficiently long samples are used, so that end effects become negligible. All measurements were carried out at constant load at 20°C. The samples were mounted vertically between grips. The upper grip was fixed in position and the lower grip was attached to the core of a linear displacement transducer. The sample extension was displayed on chart paper and also recorded on punch paper tape at regular time intervals. Each sample was tested at several nominal stresses after conditioning in the manner described below. As the loads used were never more than about 10% of the specified upper design limit of the apparatus, the machine deflection can safely be assumed to be negligible.

*Table 1* Sample details

| Sample number | Grade | $\bar{M}_n$ | $\bar{M}_w$ | $\lambda(\pm 1)$ |
|---|---|---|---|---|
| 1 | * Rigidex 50 | 6180 | 101 450 | 10 |
| 2 | * Rigidex 50 | 6180 | 101 450 | 20 |
| 3 | * Rigidex 50 | 6180 | 101 450 | 30 |
| 4 | * H020-54P | 33 000 | 312 000 | 20 |

* BP Chemicals Ltd

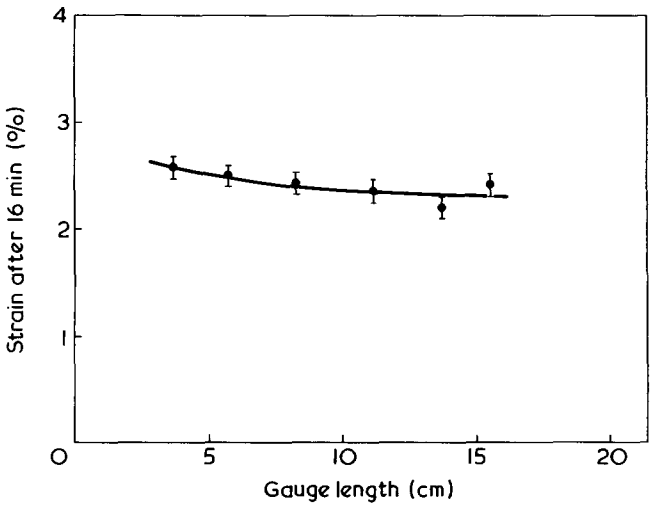


*Figure 1* Effect on the creep response of varying the sample gauge length for sample 2. The error bars correspond to the accuracy of the measurement

*Conditioning*

Preliminary measurements showed that if a sample was loaded, unloaded and relaxed, then reloaded, its creep response was smaller than it had previously been, corresponding in some cases to an apparent increase of 20–30% in the 10 sec isochronal creep modulus.

This change in behaviour has contributions arising from two sources. First, and most important, there is an irreversible, but limited, yielding or settling in the grips. This was examined by observing the effect of removing the sample after the second loading and reclamping it. During a third loading it behaved almost as though it were a fresh sample, but some small decrease in creep compliance was still observed. Repeating the test several times confirmed that nearly all the change could be attributed to grip effects. Secondly, there is a small contribution which cannot be explained in this manner and must be due to a change in the physical state of the sample as a whole. The precise nature of this change is not yet understood, but it seems likely that it arises from a small amount of permanent plastic deformation in the sample. Possible mechanisms for this conditioning process will form part of a future study, but for the present paper a standard procedure has been adopted for stabilizing the samples.

Previous work suggested[9,10] that samples can be satisfactorily conditioned by loading at the highest stress level to be employed and then unloading. In fact we found that even at the lowest stress level, and for an initial loading time of only 10 sec, a third loading gave a creep curve which coincided with that of the second. Furthermore, if the sample was loaded yet again at a higher stress level, it was found to be already conditioned. However, to ensure that there was no possibility whatsoever of problems introduced by unsatisfactory conditioning we followed our earlier procedures of always conditioning by loading at the highest stress level for 10 sec and assuming that this is sufficient to condition the samples at all lower stresses. Each sample was allowed to recover for a period of not less than ten times the loading period before being retested. The adequacy of this procedure was borne out by all subsequent experiments.

*Sample lengths*

A problem associated with the measurement of extensional strains using the method of grip displacement is that of non-uniform stress distribution along the sample length because there is always an inhomogeneous stress field in the region of clamping. The additional extension close to the grips should, however, be nearly the same for all sample lengths (for a given cross-section), so that the discrepancy in the measured strain diminishes to zero as the sample length approaches infinity. It is possible to estimate the magnitude of the effect and to determine a satisfactory gauge length by measuring the creep response of several samples identical in all respects but length. A sample similar to sample 2 was conditioned as described earlier and then loaded to 0.15 GPa for 16 min. After relaxation had been allowed to occur one grip was removed and the sample shortened by a certain amount. It was then reconditioned and reloaded. The process was repeated several times, the sample being shortened from each end alternately. The strain measured after 16 min is plotted in *Figure 1*. The error bars reflect the overall uncertainty in the measurements. It can be seen that no appreciable effect occurs for lengths in excess of about 6 cm. In all the tests reported in this paper the gauge length was therefore at least 9 cm to allow a satisfactory margin of safety.

## RESULTS AND DISCUSSION

*General features of creep and recovery behaviour*

The comparisons of creep and recovery behaviour for different samples will be chosen so as to bring out the influence of draw ratio and molecular weight as separate parameters. To demonstrate the effect of varying draw ratio, *Figure 2* shows the creep compliance as a function of time for samples 1 and 3 at three stress levels. The creep compliance is defined here as $\epsilon_c/\sigma_0$, where $\epsilon_c$ is the creep strain, and $\sigma_0$ is the applied stress. The circles represent the experimental data and the full lines are the best fits to the mathematical representation to be discussed later. Increasing the draw ratio has the effect of decreasing the compliance at all times, but does not alter the shape of the curves. With the possible exceptions of the low stress curves, a common feature is an approximately linear portion at short times followed by an upward sweep at longer time. It can be seen that the stress dependence of the creep behaviour is markedly non-linear at the longer times, particularly for low draw ratios.

The data can also be shown in another way, which is particularly instructive. In *Figure 3*, following the example of Sherby and Dorn[11] and other workers[12] the creep strain rate, $\dot{\epsilon}_c$, is plotted (on a logarithmic scale) as a function of $\epsilon_c$ for samples 1, 2 and 3 at 0.2 GPa applied stress. The full lines are derived from the best fit curves appearing in *Figure 2*.

Increasing draw ratio gives a reduction in the creep rate at any given strain, and at all three draw ratios the strain rate levels off to a constant creep rate which is markedly reduced with increasing draw ratio. This observation of a final constant creep rate is extremely important, because it suggests that there is a permanent flow process which may be superimposed on the recoverable creep, the latter being significant only at comparatively short times.

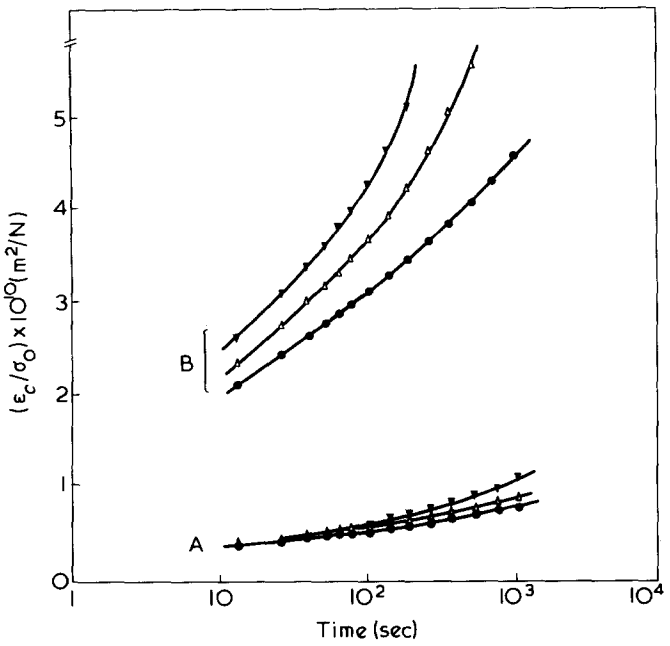


*Figure 2* Creep compliance ($\epsilon_c/\sigma_0$) of samples 1 and 3 at 0.1 (●), 0.15 (△), and 0.2 GPa (▼) applied stress ($\sigma_0$) as a function of time; (——), are least squares fits to the mechanical model. A, $\lambda = 30$; B, $\lambda = 10$

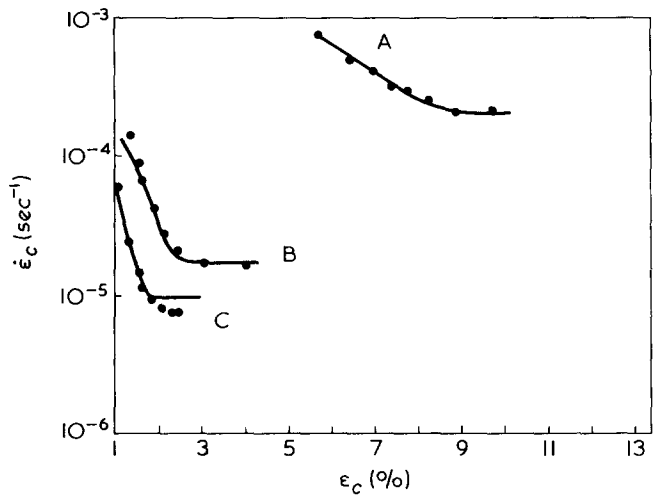


*Figure 3* Creep strain rate $\dot{\epsilon}_c$ as a function of $\epsilon_c$ at 0.2 GPa applied stress for samples 1, 2 and 3; (——), predicted by the model. A, $\lambda = 10$; B, $\lambda = 20$; C, $\lambda = 30$

In *Figures 4a, 4b* and *4c* the creep curves for samples 2 and 4 are given to show the effect of varying molecular weight at a constant draw ratio of 20. As before, the full lines are best fits to the mathematical representation. The isochronal 10 sec moduli of these samples are very similar, which is consistent with the previously reported observation that this measure of stiffness depends primarily on draw ratio[1,2,6]. The recovery data are also given for several stresses, and the broken lines are predicted from the creep data by the mathematical representation. It is significant that the range of stresses used for the two samples differs. The low molecular weight sample could not be subjected to more than 0.2 GPa before the strain rate became impracticably large, whereas the high molecular weight grade easily withstood 0.5 GPa.

The time scale has been extended somewhat at the low stresses in order to determine whether or not the curves display an upward sweep. In contrast to the high molecular weight sample, in which there is no apparent upward sweep at low stresses, the low molecular weight grade is creeping substantially at long times after loading to only 0.05 GPa. *Figure 5* demonstrates this difference over a much longer time scale and at a higher stress. Although the strain measurements were made with an optical microscope and are therefore subject to rather larger experimental error, there can be no doubt that the shapes of the curves are very

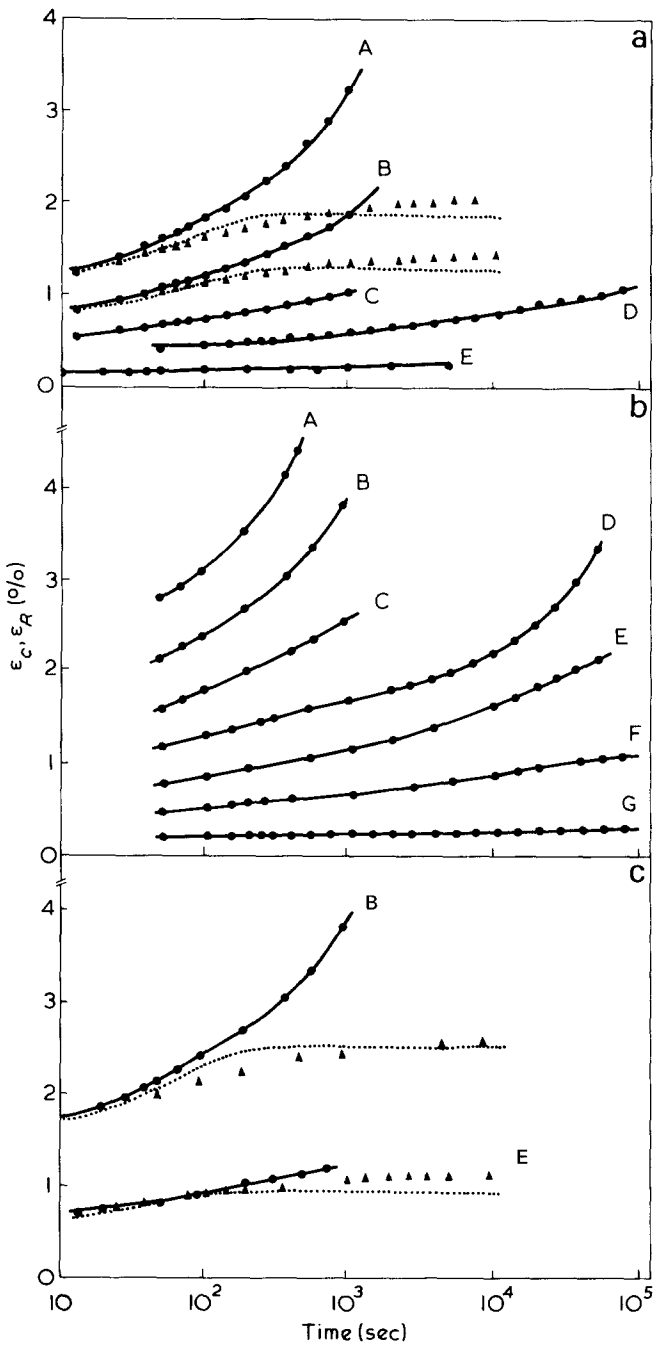


*Figure 4* $\epsilon_c$ (●) and recovery strain $\epsilon_R$ (▲) vs. time for (a) sample 2 A, 0.2; B, 0.15; C, 0.1; D, 0.05; E, 0.025 GPa and (b) and (c) sample 4: A, 0.5; B, 0.4; C, 0.3; D, 0.2; E, 0.15; F, 0.1; G, 0.05 GPa; (——), in (a) and (c) are least square fits to the mechanical model, and the dotted lines are the respective recovery curves; (——), in (b) are visual fits to the data

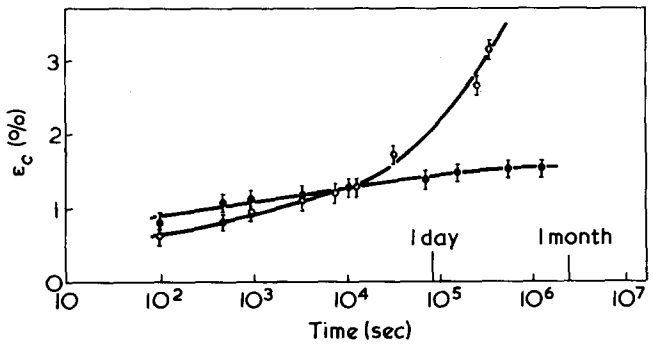


*Figure 5* A comparison of the long term creep response of samples 2(○) and 4 (●) at 0.1 GPa applied stress; (——), are visual fits and the error bars correspond to the accuracy of the measurements

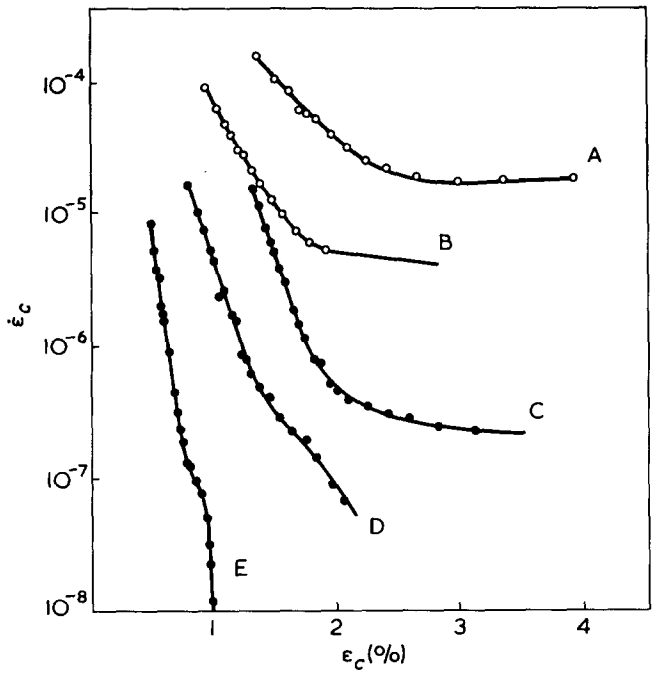


*Figure 6* $\dot{\epsilon}_c$ as a function of $\epsilon_c$ for samples 2 (○) and 4 (●); (——), are visual fits. A, 0.2; B, 0.15; C, 0.2; D, 0.15; E, 0.1 GPa

strikingly different. The stress is 0.1 GPa, and it is seen that after a few days creep in sample 4 has essentially terminated, whereas in sample 2 the creep strain is rapidly increasing.

The influence of molecular weight is also clearly seen in the Sherby–Dorn plots given in *Figure 6*. Although sample 2 displays the plateau in creep rate, $\dot{\epsilon}_c$, discussed for all the low molecular weight samples, in the high molecular weight sample 4 a plateau is apparent only at a higher stress level and even here the creep rate is about two orders of magnitude below that of sample 2 at the same stress.

Finally we note that the influence of molecular weight is also reflected in the recovery behaviour (*Figures 4a* and *4b*). In the high molecular weight sample the recovery is very nearly complete within a period of ten times the loading period at low stresses, whereas in the low molecular weight sample there is a significant amount of permanent strain for a comparable recovery time.

### *Analysis of creep and recovery data*

It is clear from these results that the creep behaviour of these materials is non-linear. A possible approach would be to model the behaviour in terms of a formal representation of non-linear viscoelasticity such as the multiple integral representation[10,13]. We have decided, however, to adopt a much less sophisticated approach, which we will show provides remarkably good insight into the physical situation. We begin by attempting to model the creep and recovery behaviour at each level of stress by the representation shown schematically in *Figure 7*. This consists of a Maxwell and Voigt element in series. $E_m$ and $E_v$ are the moduli of the Maxwell and Voigt springs respectively; $\eta_m$ and $\eta_v$ are the corresponding dashpot viscosities.

The creep strain, $\epsilon_c$, developed after a time $t$ in response to a constant applied stress $\sigma_0$ may be shown[14] to be:

$$\epsilon_c = \frac{\sigma_0}{E_m} + \frac{\sigma_c}{E_v}(1 - e^{-t/\tau}) + \frac{\sigma_0}{\eta_m} t \qquad (1)$$

where $\tau$ is the retardation time of the Voigt element, given by:

$$\tau = \eta_v / E_v$$

The data for samples 1–4 were fitted to equation (1) using a least squares procedure to obtain optimum values for the parameters $E_m$, $E_v$, $\eta_m$ and $\eta_v$. The full lines in *Figures 2* and *4* are the curves calculated from these fits and it can be seen that there is very good agreement with the experimental data. The values of the parameters obtained at each stress level are shown in *Table 2*. It can be seen that the values of $E_m$ and $E_v$ increase with draw ratio, but show comparatively small changes with stress level. This is consistent with the fact that the short time response, as determined for example from the 10 sec isochronal modulus, is linear (i.e. strain proportional to stress) and depends only on draw ratio. It also appears that $\eta_v$ is much less dependent on stress level than $\eta_m$, and it is of very great importance that the Maxwell dashpot viscosity $\eta_m$, which determines the

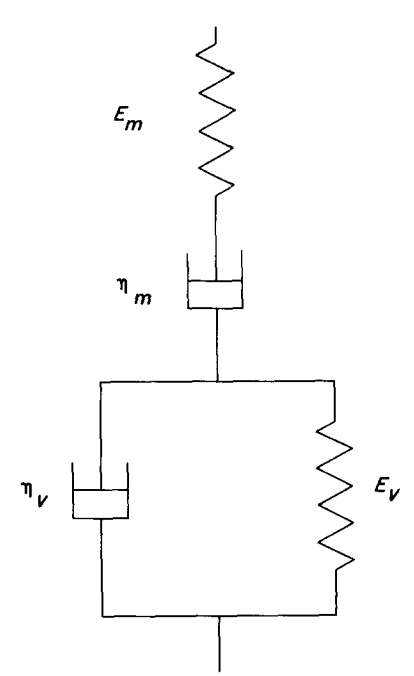


*Figure 7* Schematic representation of the four element mechanical model of creep and recovery

*Table 2* Derived model parameters

| Sample | $\sigma_0$ (GPa) | $E_m$ (GPa) | $E_v$ (GPa) | $\eta_m \times 10^{-13}$ (P) | $\eta_v \times 10^{-13}$ (P) | $\tau_v = \eta_v/E_v$ (sec) | $\tau_m = \eta_m/E_m$ (sec) | $v$ (Å$^3$) |
|---|---|---|---|---|---|---|---|---|
| 1 | 0.1 | 5.1 | 6.9 | 0.83 | 0.052 | 75 | 1627 | 98 |
| | 0.15 | 4.8 | 6.5 | 0.27 | 0.037 | 57 | 562 | |
| | 0.2 | 4.8 | 7.5 | 0.11 | 0.019 | 25 | 229 | |
| 2 | 0.025 | 17.4 | 33.5 | 18 | 0.43 | 128 | 10 344 | 87 |
| | 0.05 | 13.6 | 35.6 | 6.3 | 0.5 | 140 | 4632 | |
| | 0.1 | 17.7 | 26.4 | 3.1 | 0.22 | 83 | 1750 | |
| | 0.15 | 17.7 | 26.5 | 2.6 | 0.23 | 87 | 1468 | |
| | 0.2 | 16.4 | 26.8 | 1.2 | 0.2 | 75 | 731 | |
| 3 | 0.1 | 27.3 | 4.4 | 4.2 | 0.4 | 91 | 1538 | 64 |
| | 0.15 | 27.2 | 36.5 | 3.4 | 0.28 | 77 | 1250 | |
| | 0.2 | 25.9 | 34.9 | 2.1 | 0.25 | 72 | 810 | |
| 4 | 0.05 | – | – | – | – | – | – | 17 |
| | 0.1 | 18.3 | 31.9 | 306 | 8.66 | 2714 | 167 000 | |
| | 0.15 | 16.6 | 21.3 | 170 | 7.3 | 3427 | 102 000 | |
| | 0.2 | 15.8 | 32.7 | 77 | 3 | 917 | 48 700 | |
| | 0.3 | 25.4 | 39.1 | 4.76 | 0.28 | 77 | 1870 | |
| | 0.4 | 25 | 43 | 3 | 0.3 | 70 | 1200 | |
| | 0.5 | 21.7 | 46 | 2.5 | 0.5 | 108 | 1152 | |

irreversible creep strain in this representation, has a value which is always approximately an order of magnitude higher than $\eta_v$.

In our representation $E_m$ determines the instantaneous extension, which is immediately recovered on removal of stress, and $E_v$ and $\eta_v$ control the time-dependent recoverable creep strains. The comparatively low value of $\eta_v$ suggests that time-dependent recoverable creep strain takes place at comparatively short times after the stress is applied, whereas the irrecoverable creep dominates the long term behaviour. This is consistent with the shapes of the $\dot{\epsilon}_c$ *versus* $\epsilon_c$ curves, shown in *Figure 5*, which can be very well fitted by our representation. A more crucial test is, however, to examine the predictions of the representation for the recovery behaviour.

Equation (1) predicts that the creep strain after a time $t_f$ is:

$$\epsilon_c(t_f) = \frac{\sigma_0}{E_m} + \frac{\sigma_0 t_f}{\eta} + \frac{\sigma_0}{E_v}(1 - e^{-t_f/\tau}) \qquad (2)$$

The first term in this expression is the elastic recoverable strain in the Maxwell spring, the second term the permanent creep strain of the Maxwell dashpot and the third strain is the creep strain of the Voigt element. If the stress is removed after a time $t_f$, recovery occurs with a time constant $\tau = \eta_v/E_v$, so that for $t > t_f$ the creep strain is given by:

$$\epsilon_c'(t) = A + B e^{-(t - t_f)/\tau} \qquad (3)$$

where

$$A = \frac{\sigma_0 t_f}{\eta_m}$$

and

$$B = \frac{\sigma_0}{E_v}[1 - \exp(-t_f/\tau)]$$

We define the recovery strain at time $t$, $\epsilon_R(t)$ as the difference between the maximum creep strain (which occurs at $t = t_f$) and the final strain at time $t$. We have, for $t > t_f$:

$$\epsilon_R(t) = \epsilon_c(t_f) - \epsilon_c'(t) \qquad (4)$$

Thus, at very long times the creep strain will be just equal to $A$ and the recovery will be $\epsilon_c(t_f) - A$. In *Figure 4* the broken lines are recovery curves calculated from equation (4) using the parameters shown in *Table 2* which were determined from the creep data. These calculated recovery curves should be compared with the experimental results (shown as ▲). Although the shapes of the predicted curves are not identical to the experimentally observed recovery curves, the overall levels of recovery strains at long times are predicted very well. This confirms the usefulness of the representation with regard to separation between recoverable and non-recoverable creep. It is therefore very reasonable to proceed on the basis that $\eta_m$ represents the non-recoverable creep and to attempt to understand this component separately. We can now see that the constant creep rate at high strain seen in the Sherby–Dorn plots relates to non-recoverable creep.

The observation that the shapes of the recovery curves, as distinct from the actual level of recovery at long times, are not predicted accurately, shows that the representation of the recoverable creep by a simple Voigt element is too simple This discrepancy might be eliminated by introducing a distribution of relaxation times, which is very reasonable on physical grounds.

At this stage it is interesting to note the effect of draw ratio and molecular weight on the time dependence of the creep behaviour. Even in *Table 2* it can be seen that $\tau_v = \eta_v/E_v$ is not greatly affected by increasing draw ratio, showing that the time-dependent recoverable component is little affected. The reduction in creep with increasing draw ratio is therefore attributable mainly to an increase in $\eta_m$. Increasing molecular weight (cf samples 2 and 4) does cause an increase in $\tau_v$ as well as a very large increase in $\eta_m$. It can be concluded, however, that although increasing molecular weight does change the recoverable viscoelastic behaviour to some degree, again the major effect is on the irrecoverable

creep represented by $\eta_m$. The viscosity $\eta_m$ is a factor of a hundred higher in the high molecular weight grade at a given stress than in the low molecular weight grade. The viscosity $\eta_v$ is a factor of ten higher in the high molecular weight grade. At this juncture the discussion will therefore concentrate on attempting to obtain a more detailed understanding of $\eta_m$.

*Non-recoverable creep*

It is of particular importance to consider the non-recoverable creep component in more detail. First, this component clearly describes the permanent plastic flow and will be expected to relate to the drawing behaviour of the material. In general terms it can be appreciated that the increase in $\eta_m$ with decreasing draw ratio and increasing molecular weight corresponds to the increasing degree of strain hardening with increasing draw ratio and increasing molecular weight which has been observed in tensile drawing experiments on LPE[2]. Secondly, this non-recoverable creep is of vital importance in technological applications of ultra-high modulus LPE and may be the limiting factor in its use for fibre reinforcement of cement and other matrices.

The curve fitting procedure, with the parameterization shown in *Table 2*, indicates that $\eta_m$ is highly stress-dependent. We have therefore examined the possibility that the Maxwell dashpot should be represented by a stress activated Eyring dashpot whose creep rate is given by[15]:

$$\dot{\epsilon}_p = \dot{\epsilon}_0 \exp(-\Delta U/kT) \sinh \frac{\sigma v}{kT} \tag{5}$$

where $\Delta U$ represents the energy barrier height and $v$ is the activation volume. At high stresses the sinh term can be approximated to the exponential, and

$$\dot{\epsilon}_p = \dot{\epsilon}_0 e^{\frac{-(\Delta U - \sigma v)}{kT}} \exp[-(\Delta U - \sigma v)/kT] \tag{6}$$

It follows that:

$$\frac{\partial \ln \dot{\epsilon}_p}{\partial \sigma} = \frac{v}{kT} \tag{7}$$

Approximate values for the activation volume $v$ for samples 1–4 were obtained from the results for the highest stress levels $\sigma_1$ and $\sigma_2$ assuming:

$$\frac{v}{kT} = \frac{(\ln \dot{\epsilon}_p)_{\sigma_2} - (\ln \dot{\epsilon}_p)_{\sigma_1}}{\sigma_2 - \sigma_1}$$

and are shown in *Table 2*. It can be seen that the activation volumes for all the samples are below 100 Å$^3$. Such values contrast very greatly with those for the plastic deformation of isotropic polymers where activation volumes of the order of several thousand Å$^3$ are typical[16] and suggest large scale cooperative motions. The present results imply that permanent flow in these materials is associated with a comparatively localized molecular process. For samples 1–3 the activation volumes fall in a fairly narrow range from 98–64 Å$^3$, decreasing with increasing draw ratio. One possible molecular process would be the pulling out of chain folds by a crystal slip process in which a lattice defect such as a Reneker defect[17] travels through the crystalline regions. If we consider that the volume per event is of the order of the volume of a monomer unit of polyethylene, an activation volume of about 50 Å$^3$ is to be expected which is close to those observed for samples 1–3. In accordance with Peterlin's model of plastic deformation in LPE[18] the degree of chain folding is expected to decrease as the draw ratio increases. Further evidence for this phenomenon has been provided more recently by low frequency laser–Raman spectroscopy[19]. It is therefore reasonable to attribute the very marked decrease in creep rate with increasing draw ratio (*Figure 3*) primarily to the reduction in the total number of barrier sites available, which corresponds to a fall in the pre-experimental factor $\dot{\epsilon}_0$ in equation (6). At the highest draw ratios the indications of the original lamellar texture are very much reduced. This is consistent with the reduced sensitivity of the creep rate to draw ratio at high draw ratios, since the deformation process is then almost exhausted.

The activation volume for the high molecular weight sample is only 17 Å$^3$. This is very much lower than for all the low molecular weight samples and leads us to speculate that the molecular process is indeed different. A value of 17 Å$^3$ is much less than the unit cell volume but could correspond to a molecular process such as the pulling out of a chain entanglement or the breaking of an intercrystalline tie molecule. The structural measurements on these materials by laser Raman spectroscopy[19] show that the longitudinal acoustic mode line associated with a lamellar texture reduces to a negligible intensity in the high molecular weight samples at much lower draw rates (~10) than in the low molecular weight material, where it is of appreciable intensity even at draw ratio 20. This supports the view that the plastic deformation process is indeed different in the high molecular weight samples. Further support for this conclusion can be obtained by more detailed examination of the assumption of an activated rate process of the Eyring type. One possible approach, which is at present being examined, but involves extensive further experimental work, is to study the temperature dependence of the creep behaviour and hence obtain values for the activation energies $\Delta U$ of the plastic deformation process. Alternatively, using the presently available data, it is possible to gain further insight by the following procedure. The activation volumes were obtained at the highest stress levels for each sample, using the exponential approximation to the sinh term. It appears reasonable, as discussed above, to assume that $\dot{\epsilon}_0$ reflects only the number of barrier sites available. We therefore assume that $\dot{\epsilon}_0$ is independent of stress and calculate the sinh term appearing in equation (5) at all stress levels using our previously calculated values for the activation volume.

Taking results for samples 2 and 4, which have the same draw ratio but differ in molecular weight, it is instructive to plot the plastic strain rate (calculated from the curve fitting procedures which give the constants in *Table 2*) against $\sinh(\sigma v/kT)$ derived as above. The results are shown in *Figures 8a* and *8b*, and the broken line through the origin is the linear relationship predicted by equation (5). It is clear that in the low molecular weight sample 2, the Eyring representation of permanent plastic deformation holds over the whole range of stress. In the high molecular weight sample 4, however, this is not the case. The Eyring representation holds only at the highest stress levels, and indeed for a stress of less than about 0.2 GPa the plastic strain rate is very close indeed to zero. This result has several important consequences. First, it confirms the view expressed above that there is likely to be a difference in kind between the molecular mechanisms of permanent flow for low and high molecular weight polymers. Secondly, it suggests that we can define a critical stress, $\sigma_c$, below which a permanent

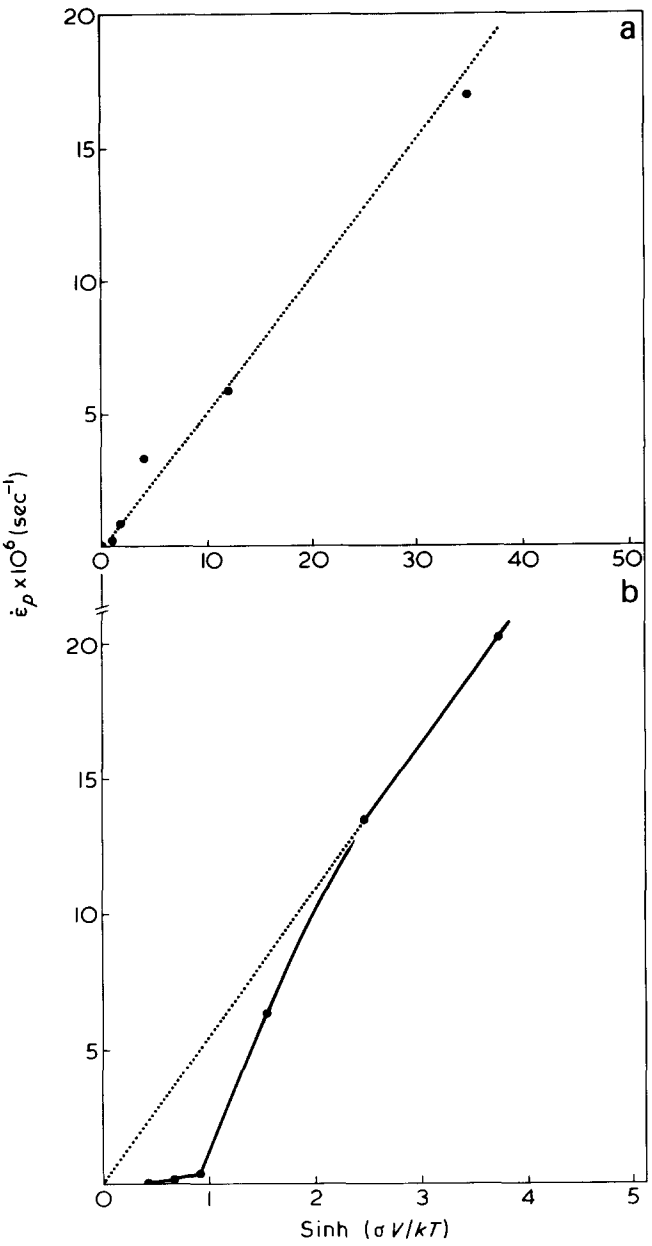


*Figure 8* Plastic strain rate $\dot{\epsilon}_p$ as a function of sinh $(\sigma v/kT)$ for (a) samples 2 and (b) sample 4. (– – –), is as suggested by equation (5); (———) in (b) is a visual fit

flow process is insignificant. This has considerable technological implications because it may define the limits of useful application of these ultra-high modulus polymers. Finally, this result suggests that an implicit equation representation for the non-linear viscoelastic behaviour along the lines previously proposed for oriented poly(ethylene terephthalate)[20] might well model the data for the high molecular weight material more accurately. As discussed in the previous publication[20] this representation predicts a critical flow stress in a formally satisfying manner.

## CONCLUSIONS

The creep and recovery behaviour of drawn polyethylenes has been fitted to a series combination of a Maxwell and a Voigt element at each level of stress. From the results it appears that the viscoelastic behaviour of these materials has two components: (a) a linear viscoelastic recoverable component; (b) a non-linear irrecoverable component which can be modelled as an activated creep process (the Eyring model).

The recoverable viscoelastic behaviour is not greatly affected by draw ratio or molecular weight, apart from a considerable increase in the level of stiffness with increasing draw ratio, as is now well known.

The irrecoverable creep component is, however, affected in a dramatic fashion by both draw ratio and molecular weight. For lower molecular weight samples, the reduction in irrecoverable creep with increasing draw ratio can be attributed to gradual exhaustion of the barrier sites as the initial lamellar texture of the material is removed. The high molecular weight sample, on the other hand, shows a critical stress for irrecoverable creep, as well as a much smaller activation volume for the creep process. It therefore seems likely that there is a different mechanism of creep in this case. This result brings out the essential continuity between the creep behaviour and the drawing behaviour. We have already emphasized[2] that the drawing behaviour of these materials is best understood in terms of a molecular network, where both physical entanglements and crystalline regions can form network junction points. In the low molecular weight materials the crystalline regions form the majority of the network junction points, but the situation is reversed for high molecular weight materials where physical entanglements play the dominant role. This explains the striking effect of initial morphology on the drawing behaviour of low molecular weight linear polyethylene, compared with the drawing of high molecular weight polymers where only molecular weight affects the behaviour. Viewing the irrecoverable creep as an extension of draw, which seems reasonable as both relate to permanent plastic deformation, now consider the findings of the present investigation. On this basis we would anticipate that the irrecoverable creep of the low molecular weight polymer relates to a crystal deformation process, such as the pulling out of chain folds by a crystal slip process, but that creep of the high molecular weight polymer relates to a localized molecular process such as the breaking of an intercrystalline tie molecular or the pulling out of a chain entanglement. In the low molecular weight materials the network can deform further by irreversible plastic deformation of the crystalline regions. In the high molecular weight materials the network relates primarily to physical entanglements and further deformation requires either that these be destroyed or that chain scission occurs.

## REFERENCES

1 Capaccio, G. and Ward, I. M. *Nature (Phys. Sci.)* 1973, **243**, 130, 143; *Polymer* 1974, **15**, 233; *Polym. Eng. Sci.* 1975, **15**, 219; *Br. Pat. Application* 10 746/73 (filed 6 March 1973)
2 Capaccio, G., Crompton, T. A. and Ward, I. M. *Polymer* 1976, **17**, 644; *J. Polym. Sci. (Polym. Phys. Edn)* 1976, **14**, 1641
3 Gibson, A. G., Ward, I. M. Cole, B. N. and Parsons, B. *J. Mater. Sci.* 1974, **9**, 1193
4 Gibson, A. G. and Ward, I. M. *Br. Pat Application* 30 823/73 (filed 28 June 1973)
5 Smith, J. B., Davies, G. R., Capaccio and Ward, I. M. *J. Polym. Sci. (Polym. Phys. Edn)* 1975, **13**, 2331
6 Andrews, J. M. and Ward, I. M. *J. Mater. Sci.* 1970, **5**, 411
7 Capaccio, G. and Ward, I. M. *Third International Conference on Deformation, Yield and Fracture of Polymers, Churchill College, Cambridge,* 1976
8 Morgan, C. J. and Ward, I. M. *J. Mech. Phys. Solids* 1971, **19**, 165
9 Leaderman, H. 'Elastic and Creep Properties of Filamentous Materials and other High Polymers', The Textile Foundation, Washington, DC 1943

10 Ward, I. M. and Onat, E. T. *J. Mech. Phys. Solids* 1963, **11**, 217
11 Sherby, O. D. and Dorn, J. E. *J. Mech. Phys. Solids* 1956, **6**, 145
12 Mindel, M. J. and Brown, N. *J. Mater. Sci.* 1973, **8**, 863
13 Green, A. E. and Rivlin, R. S. *Arch. Rat. Mech. Anal.* 1957, **1**, 1
14 Ward, I. M. 'Mechanical Properties of Solid Polymers', Wiley, London, 1971, p 91
15 *Ibid* p 205
16 Haward, R. N. and Thackray, G. *Proc. Roy. Soc. (A)*, 1968, **302**, 453
17 Reneker, D. H. *J. Polym. Sci.* 1962, **59**, 539
18 Peterlin, A. *J. Mater. Sci.* 1971, **6**, 490
19 Capaccio, G., Ward, I. M. and Wilding, M. A. in preparation
20 Brereton, M. G., Croll, S. G., Duckett, R. A. and Ward, I. M. *J. Mech. Phys. Solids* 1974, **22**, 97